Electronic Structure of Elemental Calcium and Zinc

Theodore D. Brennan and Jeremy K. Burdett*

Department of Chemistry and James Franck Institute, The University of Chicago, Chicago, Illinois 60637

Received August 7, 1992

The results of tight-binding calculations on elemental calcium (d^0s^2) and elemental zinc ($d^{10}s^2$) show that the anomalous ρ vs pressure behavior observed for calcium and the anomalous c/a ratio for zinc are due to the presence of an avoided crossing between s and p levels in calcium and the lack of the same crossing in zinc. The avoided crossing in calcium (an effect initially suggested by Mott) causes the Fermi surface to contract with increasing pressure resulting in a decrease in conductivity. (The full electronic picture is more complex since d orbitals need to be included in the calculation to obtain the correct Fermi surface.) The lack of avoided crossing in zinc means that the top of the "s band" is antibonding between the close-packed layers of the ideal hexagonal structures leading to an increased c/a ratio > (c/a) ideal.

All materials are predicted to become metallic under pressure, although for some of them the pressures involved (over 2.5 Mbar for hydrogen[1]) are very large. This occurs quite simply because energy bands broaden as the interatomic separation decreases and the relevant interaction or hopping integrals which determine the width increase. Thus elemental calcium (fcc), strontium (fcc), and barium (bcc) are somewhat unusual because their conductivity decreases under pressure.[2] The conductivity of Sr decreases by a factor of six times up to ~36 kbar after which the conductivity starts to increase again.[3] The conductivity of Ca decreases 60-fold up to 370 kbar after which it begins to increase again.[4] The traditional tight-binding explanation for this phenomenon suggested first by Mott is an avoided crossing between s and p orbitals.[5] The actual details of the Fermi surface and how this comes about have been the subject of several good electronic structure calculations.[6] While the d^0s^2 metals show interesting behavior under pressure, the $d^{10}s^2$ metals show unusual structural distortions. Both Zn and Cd deviate from the ideal c/a ratio for a hexagonal close packed structure. Hcp structures are classified according to their c/a ratio: ϵ-hcp c/a = 1.55–1.58, ζ-hcp c/a = 1.63 (ideal hcp), and η-hcp c/a = 1.77–1.88. Zn and Cd are η-hcp structures with c/a ratios of 1.856 and 1.886. Previous studies have addressed the change of the Fermi surface as the c/a ratio changes and the dependence of structure type on electron count. Recent calculations[7] using second moment scaled[8] Hückel calculations correctly predict the preferred structure of most of the transition metals and main group elements and confirm Hume-Rothery's electron concentration rules. These calculations including d orbitals correctly predict that at $12e^-$/atom (i.e. zinc) the preferred structure is the η-hcp phase. In this paper we will investigate the reasons behind the anomalous c/a ratio found in zinc which none of the previous band structure calculations have addressed and the reasons behind the behavior of both d^0s^2 and $d^{10}s^2$ metals under pressure.

Avoided Crossings of Orbitals

Imagine a one dimensional chain of atoms (running along x) each carrying an s and p_x orbital. The dispersion of the s band is expected to increase in energy with **k** and the p band drop in energy, simply as a result of the difference in parity of the two orbitals (**1**). However if the s–p separation ($\alpha_s - \alpha_p$) is small

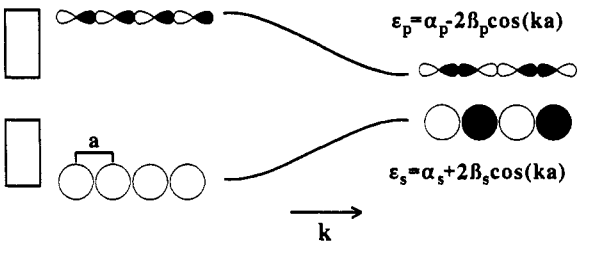

1

compared with the size of s–p overlap (β_{sp}) then the two curves will cross somewhere along **k**. In fact an avoided crossing will take place as a result of this s–p mixing. We can highlight some of the important factors by study of the electronic structure of a linear chain of atoms. For widely separated atoms the highest s state lies below the lowest p state. As the atoms are brought closer together the s and p bands mix (β_{sp} increases) so that the top of the lower band becomes p-like and the bottom of the upper band becomes s-like generating an avoided crossing. The dependence of the effect on the size of the energy gap between the s and p levels is shown, for example by Ca (~2 eV gap) and Zn (~4 eV gap). Using the M–M distances found for the metals, a linear chain of Ca atoms is found to have an avoided crossing while Zn with a larger s–p gap does not, as shown in Figure 1. The calculations used the extended-Hückel implementation of tight-binding theory with parameters given in the Appendix. Finally, contracting the orbitals by changing the Slater coefficients yields an effect similar to changing the internuclear distance.

Band Structure of Elemental Ca

The effect of the band structure of changing the Ca–Ca distance for a linear chain of Ca atoms along the x coordinate without d

* To whom correspondence should be addressed at the Department of Chemistry, The University of Chicago.

(1) Mao, H.-K.; Hemley, R. J. *Am. Sci.* **1992**, *80(3)*, 234.
(2) Bundy, F. P.; Strong, H. M. *Solid State Phys.* **1962**, *13*, 81.
(3) Bridgeman, P. W. *Proc. Am. Acad. Arts Sci.* **1952**, *81*, 165.
(4) Balchan, A. S.; Drickamer, H. G. *Rev. Sci. Instrum.* **1961**, *32*, 308.
(5) Mott, N. F. *Metal Insulator Transitions*; Barnes & Noble Books: New York, 1974.
(6) (a) Manning, M. F.; Krutter, H. M. *Phys. Rev.* **1937**, *51*, 761. (b) Harrison, W. A. *Phys. Rev.* **1960**, *118*, 1190; **1963**, *131*, 2433. (c) Chatterjee, S.; Chakraborti, D. K. *J. Phys. C: Met. Phys. Suppl.* **1970**, *3*, S120. (d) Altmann, S. L.; Cracknell, S. P. *Proc. Phys. Soc.* **1964**, *84*, 761. (e) Vasvari, B.; Animalu, A. O. E.; Heine, V. *Phys. Rev.* **1967**, *154*, 535. (f) Altmann, S. L.; Harford, A. R.; Blake, *J. Phys. F: Met. Phys.* **1971**, *1*, 791. (g) Ross, M.; Johnson, K. *Phys. Rev. B* **1970**, *2*, 4852. (h) Williams, R. W.; Davis, H. L. *NBS Spec. Publ. 323* **1971**, 57. (i) Ballinger, R. A.; Allen, B. R. *J. Phys. F: Met. Phys.* **1975**, *5*, 1135. (j) Jan, J.-P.; Skriver, H. L. *J. Phys. F: Met. Phys.* **1981**, *11*, 805.
(7) (a) Lee, S. *Acc. Chem. Res.* **1991**, *24*, 249. (b) Lee, S. *J. Am. Chem. Soc.* **1991**, *113*, 101, 8611. (c) Hoistad, L. M.; Lee, S. *J. Am. Chem. Soc.* **1991**, *113*, 8216.
(8) (a) Pettifor, D. G.; Podloucky, R. *Phys. Rev. Lett.* **1984**, *53*, 1080. (b) Burdett, J. K.; Lee, S. *J. Am. Chem. Soc.* **1985**, *107*, 3063.

0020-1669/93/1332-0746$04.00/0

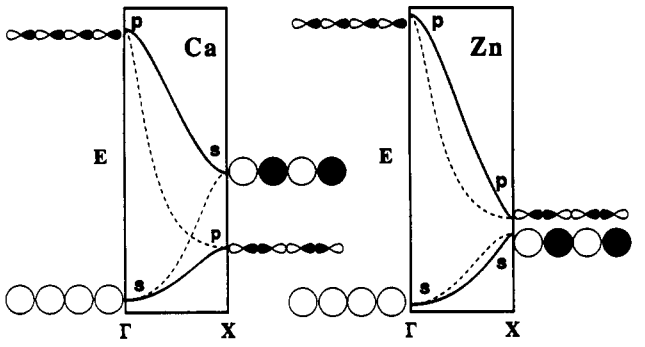

Figure 1. Band structure for linear chain of Ca (left) and Zn (right) atoms s and p_x orbitals only. The dashed lines represent unhybridized bands; the solid lines, hybridized bands. Note the avoided crossing observed for Ca but not for Zn.

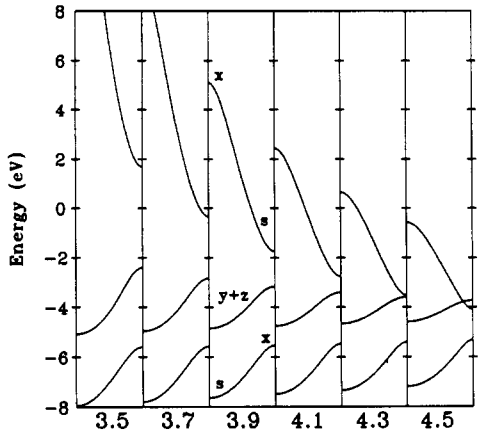

Figure 2. Band structure for a linear chain of Ca atoms, s and p orbitals only, for Ca–Ca distances 3.5–4.5 Å. The labels s, x, y, and z represent the character of the bands. The equilibrium distance observed in elemental Ca is 3.95 Å.

orbitals is seen in Figure 2. As one expects the p_y and p_z orbitals which are perpendicular to the chain are mostly non-bonding with a smaller band dispersion than p_x or s. The lowest band has s bonding character at the bottom and p_x bonding at the top of the band, while the upper band has p_x antibonding character at the top and s antibonding character at bottom—the signature of the avoided crossing. So reducing the internuclear separation should lead to a drop in energy at the top of the "s band" (the lower band) and an increase in energy of the bottom of the "p band" (the higher energy band). As the Ca–Ca internuclear distance is reduced, the calculated gap between the top of the lowest band and the bottom of the upper band increases as a result. This corresponds qualitatively to the effect observed in Ca metal that we will see later. Recall that as the pressure increases, thereby reacting the internuclear distance, the conductivity decreases. From Figure 1 we note that as the Ca–Ca distance decreases, the top of the lower band drops only slightly while the bottom of the upper band rises dramatically both with and without inclusion of d orbitals in the calculation.

The band structure of fcc Ca metal with s and p orbitals is shown in Figure 3. The character of the bands at the symmetry points is given with the labels s, x, y, and z corresponding to s, p_x, p_y, and p_z character with a "/" denoting the character of degenerate bands. Importantly, when the same calculation is repeated for zinc the appearance of the dispersion plot is very similar. There is, of course, a shift in the energy scale but the most significant difference is the change in the character of the first and second bands at point L (2).

L is the point ($^1/_2$, $^1/_2$, $^1/_2$) along the direction perpendicular to the close packed layers. In Ca L_1 has xyz character and L_2 has s character while in Zn L_1 has s character and L_2 xyz. Thus in Ca metal going from Γ to L there is an avoided crossing

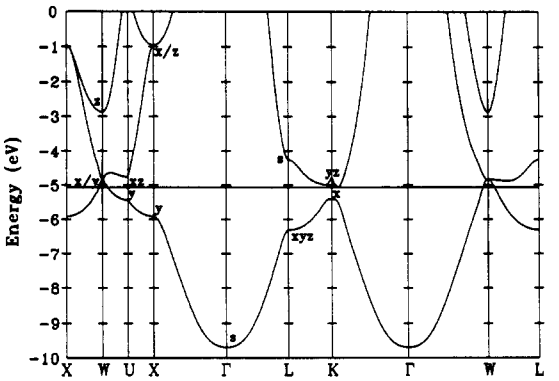

Figure 3. Band structure for Ca fcc metal s and p orbitals only. The band character at symmetry points is denoted by s, x, y, and z labels. The slashes "/" denote degeneracy.

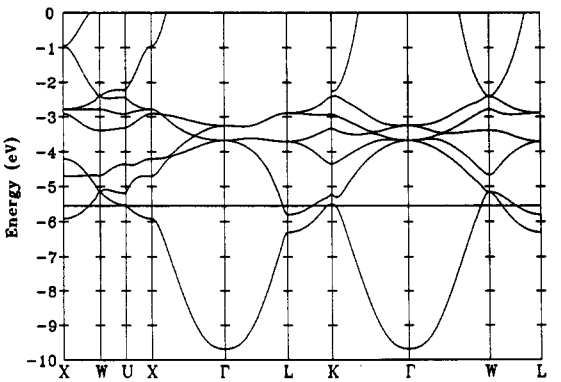

Figure 4. Band structure for Ca fcc metal s, p, and d orbitals included.

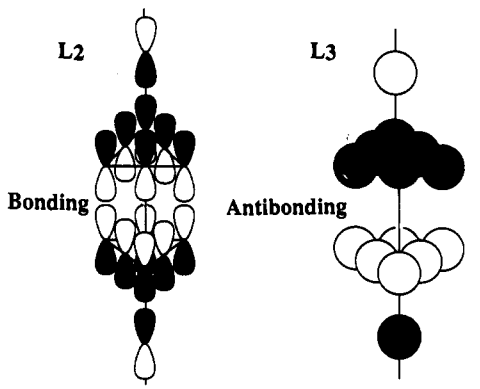

2

analogous to that discussed above for the linear chain. When the lattice is compressed, corresponding to higher pressure, we expect to see a similar effect at L in the Ca metal band structure to that seen in the Ca linear chain. As the V/V_0 ratio is reduced, we expect L_1 to drop slightly while L_2 is pushed up in energy. Before seeing how this changes the Fermi surface we need to add d orbitals to this picture.

The band structure for Ca fcc metal with the inclusion of d orbitals is shown in Figure 4. This calculation compares well with that of Altmann et al.[6f] and Jan and Skriver[6j] with the exception of the first three bands at W. In Figure 4, the first two bands at W are degenerate whereas Altmann et al. and Jan and Skriver show that the second and third bands are degenerate. A careful study of the band character at W shows that this discrepancy can be removed by a small change in th VSIP for Ca 3d giving the band structure shown in Figure 5a.

The pressure dependence of the conductivity of calcium metal is now easy to see by comparing the band structure of the metal by isotropically compressing the lattice with V/V_0 ratios of 1.0, 0.86, and 0.6 corresponding to normal pressure, ~30kbar, and

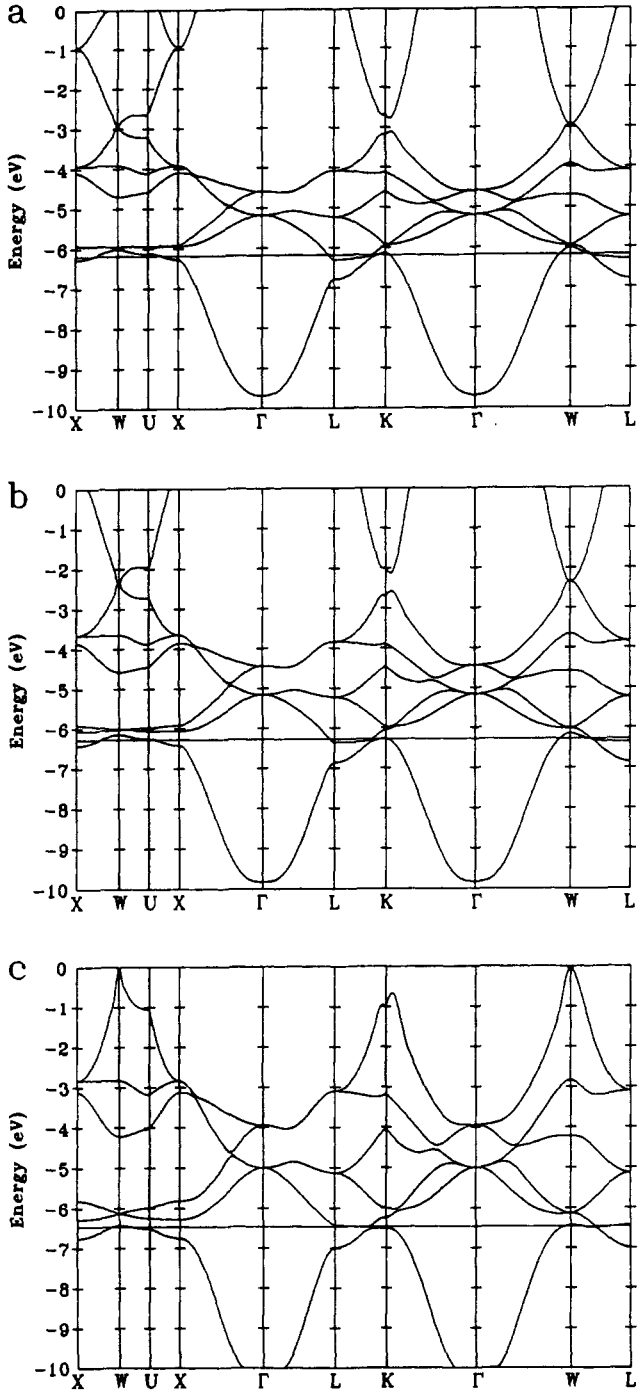

Figure 5. Band structure for Ca fcc metal, s, p, and d model with adjusted d levels as a function of lattice volume: (a) $V/V_0 = 1.0$; (b) $V/V_0 = 0.86$; (c) $V/V_0 = 0.6$.

~300kbar as shown in Figure 5a–c. Comparing Figures 5a and 5c we see that at high pressure the hole surface has disappeared at U and K and nearly disappeared at W and the electron surface at L has disappeared. Calcium is now in a semimetallic state with the conduction and valence bands having barely any overlap at the Fermi surface. A significant part of the change has been associated with the change in behavior at L where the bands "repel" on squeezing.

Band Structure of Elemental Zn

The band structure of zinc with the observed η-hcp structure is shown in Figure 6a. Because there are two atoms per unit cell in the hcp structure rather than one in the fcc structure, the Γ to A direction in hcp is equivalent to a folding of the Γ to L direction of fcc electronic structure. The lack of avoided crossing

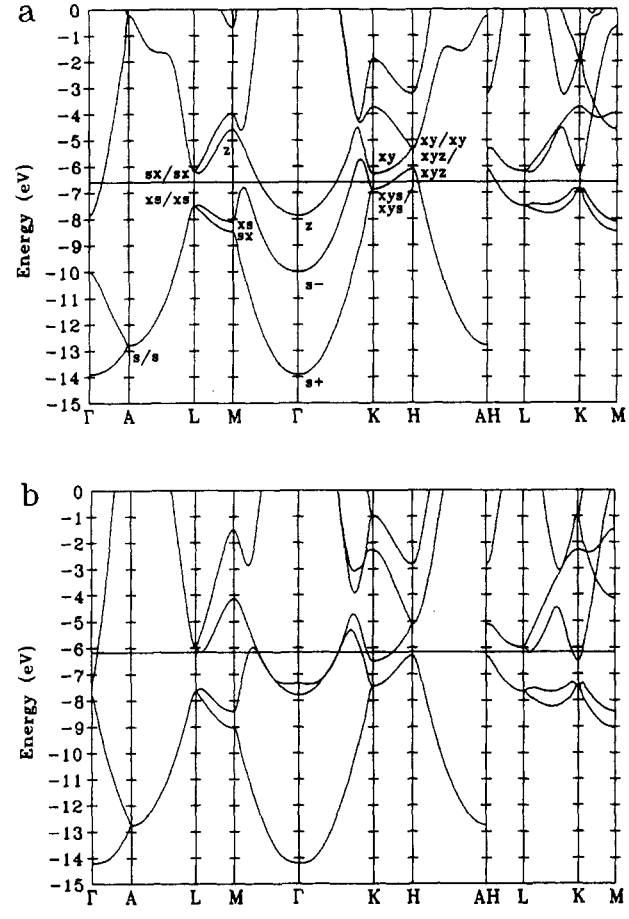

Figure 6. Band structure for Zn hcp metal with (a) $c/a = 1.856$, the observed structure, and with (b) $c/a = 1.63$, the ideal structure. Note that the second band at Γ has shifted dramatically.

between s and p bands that was observed at L in the hypothetical Zn fcc structure appears in the hcp electronic structure at Γ. The lack of avoided crossing results in Γ_2 being s antibonding in character (s–) and Γ_3 being p_z bonding. Upon compression along the c axis to give the ideal hcp c/a ratio 1.63, the most dramatic change occurs in the second band at Γ, Figure 6b. As the close packed layers are brought together to give the ideal hcp structure, the Γ_2 band is pushed up in energy, destabilizing the structure. This is exactly the solid state analog of the repulsion of two s^2 He atoms when brought together. Thus, the observed phase for elemental Zn is η-hcp where the close packed layers have been pushed apart because of the antibonding contribution at Γ. If the a axis is held fixed for Zn (Zn–Zn bond distance 2.664 Å) and the c axis varied, the total energy calculated using the extended-Hückel scheme with s and p orbitals is minimized with a Zn–Zn distance between the layers of 3.1 Å as compared to the observed value of 2.913 Å. This result is in accord with the predictions of the model. In more general terms the experimentally observed structure changes from ζ, ϵ hcp (with c/a values either equal or less than the ideal value) to the η hcp arrangement (where c/a is greater than the ideal) as the number of electrons increases and the s band becomes filled. This result, in accord with the ideas developed here, was shown theoretically in a study by Hoistad and Lee.[7c]

The difference between Ca and Zn can be understood by examining the bond overlap populations for hypothetical Ca and Zn ideal hcp structures, Figure 7. At the Fermi level in the electronic structure of Ca, s band mixing with the low-lying, empty d bands results in a bonding situation for both the intra- and inter-layer Ca–Ca interactions. Zn with filled d bands and a wide s–p gap has a bonding interaction for intra-plane Zn–Zn and anti- or non-bonding Zn–Zn interactions between the close

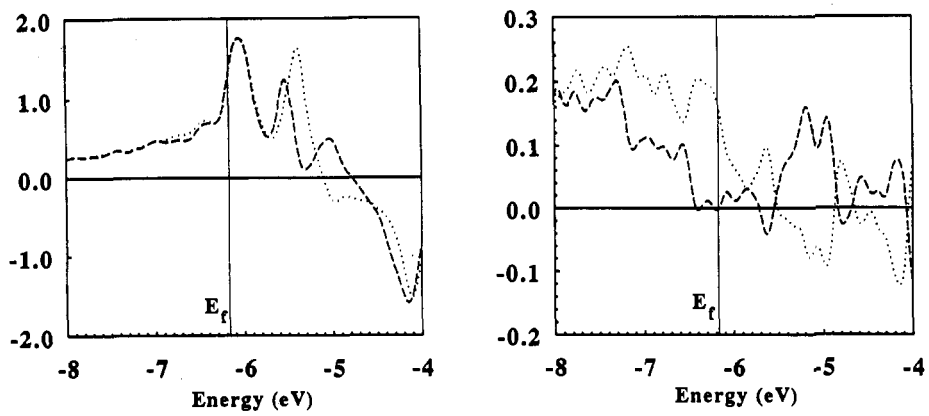

Figure 7. Bond overlap populations (COOP) for Ca (left) and Zn (right) ideal hcp structure as a function of energy. The dotted lines are the overlap population for the in-plane bonds and the dashed line is that for the between close packed layer bonds. A positive value indicates a bonding interaction.

packed layers at the Fermi level. The difference simply arises through the differences in s/p mixing the two systems.

Conclusions

Using really quite simple arguments, akin to the early ones of Mott, we have shown that the pressure dependent conductivity of Ca and the large c/a ratio in Zn can be understood by an avoided s–p band crossing in Ca and no such s–p crossing in Zn. However, the situation is a little more complex in detail. Inclusion of d orbitals is necessary to reproduce the proper Fermi surface for Ca and to predict the correct structure type for elemental Ca and Zn when using the Hückel method in conjunction with second moment scaling. An interesting observation is that the extended-Hückel tight-binding calculations give band structure results comparable to other methods of calculation even for the alkaline earths. The success is reassuring and encourages continued computation with alloys and surfaces from this part of the periodic table.

Acknowledgment. This research was supported by the National Science Foundation under NSF Grant DMR-88-09854.

Appendix

The H_{ii} parameters for Ca^0 and Zn^0 were calculated from standard atomic spectra tables[9] setting the valence shell ionization potential equal to the ground state ionization potential plus the promotion energy for the cation minus the promotion energy for the neutral atom[10]: $VSIP = I_g + P^+ + P^0$. Slater coefficients for calcium[11] and zinc[12] were taken from standard sources. The Slater coefficients for the Ca and Zn d levels were taken as an extrapolation of the first row transition metal d parameters. The H_{ii} and Slater coefficients used in this paper are listed in Table I. The extended-Hückel[13] tight-binding[14] calculations were done using the program EHMACC.[15]

Table I. Atomic Parameters

orbital	ζ_1	c_1	ζ_2	c_2	H_{ii}
Ca 4s	1.2				−6.111
Ca 4p	1.2				−4.219
Ca 3d	4.0	0.4	1.3	0.7	−3.541 (−5.0)[a]
Zn 4s	2.01				−9.391
Zn 4p	1.70				−5.163
Zn 3d	6.15	0.59	2.60	0.57	−17.302

[a] Adjusted to match previously calculated band structure calculations.[6f,j]

(9) Moore, C. E. Atomic Energy Levels. *Natl. Stand. Ref. Data Ser.* **1971**, *35*.
(10) Mulliken, R. *J. Chem. Phys.* **1934**, *2*, 782.
(11) Zheng, C.; Hoffmann, R. *J. Am. Chem. Soc.* **1986**, *108*, 3078.
(12) Silvestre, J.; Albright, T. A. *Isr. J. Chem.* **1983**, *23*, 139.
(13) (a) Hoffmann, R. *J. Chem. Phys.* **1963**, *39*, 1397. (b) Hoffmann, R.; Lipscomb, W. N. *J. Chem. Phys.* **1962**, *36*, 2179, 3489; *37*, 2872.
(14) (a) Whangbo, M.-H.; Hoffmann, R. *J. Am. Chem. Soc.* **1978**, *100*, 6093. (b) Whangbo, M.-H.; Hoffmann, R.; Woodward, R. B. *Proc. R. Soc. London, Ser. A* **1979**, *366*, 23.
(15) The program EHMACC was produced by M.-H. Whangbo, M. Evain, T. Hughbanks, M. Kertesz, S. Wijeyesekera, C. Wilker, C. Zheng, and R. Hoffmann.